



# Equilibrium position for a particle in a horizontal shear flow

Zhi-Gang Feng, Efstathios E. Michaelides \*

*Department of Mechanical Engineering, School of Engineering and Center for Bioenvironmental Research,  
Tulane University, New Orleans, LA 70118-5674, USA*

Received 8 January 2001; received in revised form 30 March 2003

---

## Abstract

The lift on a particle that is caused by its proximity to a boundary and the equilibrium position of this particle in a linear shear flow have been studied using the lattice Boltzmann method. The shear particle Reynolds numbers examined were in the range 0–18 and the particle to fluid density ratios were in the range 1.005–1.1. We have found that heavy particles will deposit at the bottom of the channel, while lighter particles remain suspended and attain an equilibrium vertical position, which is characterized by the equality of the lift and the gravity forces. At this equilibrium distance from the boundary, the vertical velocity component is zero, while the horizontal and rotational velocities of the particle are finite. For circular particles, we have found out that the equilibrium position is independent of the initial height of release of the particles and depends only on the density ratio of particle to fluid and the shear Reynolds number. The particle equilibrium positions for the linear shear flow are compared with those computed for Poiseuille flow conditions. Based on the numerical simulation results, a correlation has been derived between the particle-fluid density ratio and the critical particle Reynolds numbers needed to lift the particles. The effects of particle rotation and shape on the equilibrium position have also been studied by simulating the motion of rectangular particles.

© 2003 Elsevier Science Ltd. All rights reserved.

---

## 1. Introduction

Most of the studies related to the lift force on a solid surface are mainly the subject of aerodynamics. In the case of particulate flows and sediment studies, it is understood that certain phenomena associated with the lift forces on particles are important in the migration of particles

---

\* Corresponding author. Tel.: +1-504-865-6457; fax: +1-504-862-8747.  
E-mail address: [emichael@tulane.edu](mailto:emichael@tulane.edu) (E.E. Michaelides).

from walls, the fluidization of a bed of particles, the re-distribution of particles in shear flows and as one of the mechanisms that causes the re-suspension of particles from the bottom of a conduit.

Regarding particulate flows close to walls, the older studies mainly focus on experimental methods and produced a good number of experimental results, such as those by Segre and Silberberg (1961, 1962) who found that neutrally buoyant particles released off center in a pressure-driven pipe flow, will not migrate to the pipe center-line, but instead will find an equilibrium position at about 0.6 radii off the center-line. The numerical simulations by Feng et al. (1994) resulted in the same conclusion for a circular particle in a two-dimensional flow. Saffman (1965) conducted the first analytical study on the lift exerted on a sphere by a shear flow and derived a formula for this lift, which is applicable at low Reynolds numbers and far from all boundaries. McLaughlin (1993) studied the cases of a sphere in a wall-bounded linear shear flow in which the flow outer region influences the lift force to the leading order. More recently, there are several new studies on the lift force of a two-dimensional particle in Couette and Poiseuille flow by Joseph and his co-workers (Joseph and Ocano, 2002; Joseph, 2002; Patankar et al., 2001). They developed the “Arbitrary-Lagrangian-Eulerian” numerical method with body-fitted unstructured finite elements, which is capable to compute the particle and flow interaction problems. More details on this method and the problems solved may be found in Patankar et al. (2001). Also Kurose and Komori (1999) studied the lift forces on a rotating sphere in a linear shear flow. They calculated the lift coefficient for a stationary sphere and found that it rapidly decreases with increasing particle Reynolds number. Actually at particle Reynolds number greater than 60, the lift coefficient becomes negative and they attribute this to the flow separation behind the particle.

In his Ph.D. thesis, Zhu (2000) studied the equilibrium position of a circular particle in Couette flow and derived results that show the equilibrium position as a function of the particle Reynolds number at particle/fluid density ratio in the range 1.001–1.01. The results were obtained at relatively low particle Reynolds numbers ( $Re_p < 5$ ). Patankar et al. (2001) did a more detailed study on the equilibrium position of a circular particle in a pressure-driven Poiseuille flow using the finite element method, and derived a general data structure for the interrogation of the numerical simulations to be used in developing a theory of fluidization by lift due to the motion of the fluid.

In this paper, we use the lattice Boltzmann method (LBM) to examine the transient motion of a particle released from rest and to determine the vertical equilibrium position of circular and rectangular two-dimensional particles in simple shear flow at Reynolds numbers up to 18. In a previous study on particle resuspension (Feng and Michaelides, 2002a,b) we have found that suspended particles close to a boundary would influence considerably the forces (drag and lift) of stationary particles, which are at rest in the bottom of the channel. In this study, we try to determine when the particles would settle or remain suspended in the flow at an equilibrium height. The main parameters in this study are the particle Reynolds number and the density ratio. We also study the effect of the initial gap between a rectangular particle and the channel bottom to the motion of the particle and its equilibrium position.

## 2. Simulation method

The LBM has been discussed in detail in many articles (Ladd, 1994a,b; Chen and Doolen, 1998; Feng and Michaelides, 2002a). It is a computational method based on a microscopic fluid model

and is ideally suited for calculations of fluid-particle interactions where multiple particles are involved. The LBM originated from the lattice gas (LG) automata, a discrete particle kinetics method similar to Boltzmann's kinetic theory of gases. The LG automata utilize a discrete lattice and discrete time. It consists of two distinct processes, collision and propagation. Frisch et al. (1986) are considered the first to apply this method to computational fluid dynamics and to have recovered accurate solutions to the Navier–Stokes equations from computations based on an early version of the LBM. In this method the fluid particles are assumed to reside on a uniform simple orthogonal lattice (the most common configuration), and move from each node to its neighbor nodes during the discrete time step. The no slip boundary condition on the solid particle or the solid wall includes the so-called “bounce-back” rules (Ladd, 1994a,b). The force and torque on each particle are computed by summing the individual force and torque at each solid node. In order to smooth the forces and torques, these components are averaged over two time steps and then used to update the particle velocity and position with simple time integration (Ladd, 1994a,b). A more detailed presentation of this method as applied to boundaries and groups of particles may be found in our two previous papers (Feng and Michaelides, 2002a,b). The results of these papers were validated by similar results based on the finite element method.

### 3. Results and discussion

We simulate a single suspended two-dimensional particle in two-dimensional Couette flow as depicted in Fig. 1. The particle is initially being held at rest and at  $t = 0$  it is released inside the flow domain. The direction of gravity is perpendicular to the flow direction and the particle is slightly heavier than the fluid. Periodic boundary conditions are assumed at the inlet and the outlet of the flow domain. The channel height is  $H$  and its width is  $W$ . Allowing the upper plate to move with constant velocity  $U_w$  while keeping the lower plate stationary creates the linear shear flow. Thus, the shear rate  $G$  is  $U_w/H$ .

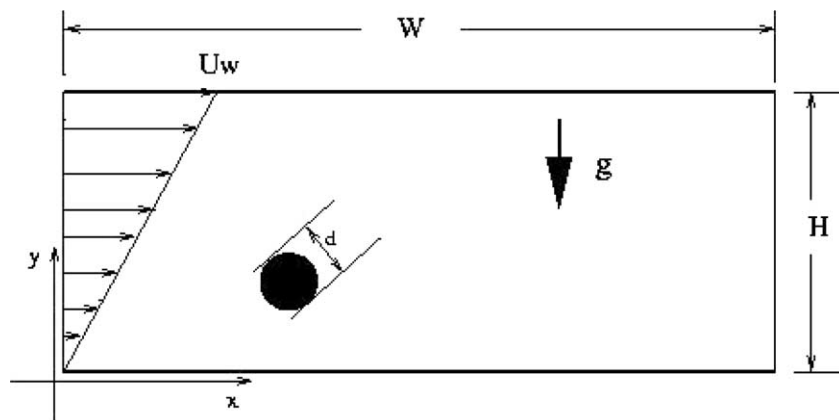


Fig. 1. Schematic diagram of a particle in a shear flow.

The following dimensionless parameters, which are used in the results of the simulations:

Channel Reynolds number:

$$Re_C = \frac{\rho_f U_W H}{\mu_f}$$

Particle shear Reynolds number:

$$Re_p = \frac{\rho_f G d^2}{\mu_f}$$

Particle gravity Reynolds number:

$$Re_G = \frac{\rho_f V_g d}{\mu_f}$$

Particle to fluid density ratio:

$$\sigma = \frac{\rho_p}{\rho_f}$$

In the definition of particle gravity Reynolds number,  $V_g$  is the terminal velocity of the particle when it settles in an infinite fluid. It is given by the expression:

$$V_g = \frac{(\sigma - 1)\rho_f g d^2}{\mu_f} \quad (1)$$

For the numerical simulations, unless otherwise specified, we have generally used the following dimensions: particle diameter 20 lattice units, channel height 200 lattice units and channel width 400 lattice units. From grid validation studies and our previous results (Feng and Michaelides, 2002a) we have found that these values for the flow domain and for the particle diameter yield accurate results for the forces on the particles and their equilibrium positions. The fluid density is equal to 1 and the density of the particle was a variable, close to 1. For most of the cases, the fluid viscosity is chosen to be 1/30 in lattice units. This choice and the ones on the density of the particle have resulted in particle shear Reynolds numbers in the range from 2 to 20.

### 3.1. Equilibrium positions of particles with different density ratios

Particles with  $\sigma > 1$  are released in the shear flow from rest at a certain height. In the absence of flow, one expects these particles to settle in the bottom. However, the shear flow creates a lift and the proximity to the wall amplifies this lift on the particles. For a particle that is slightly heavier than the fluid, the particle lift may be high enough for the particle to migrate away from the bottom. Thus, the particle will flow at an equilibrium height, the “equilibrium position” from the bottom, where the combined lift of the shear and the proximity to the bottom wall is equal to the apparent weight of the particle.

We computed the flow trajectories of several particles for a long time and determined the final equilibrium positions of two-dimensional particles in the range  $1.005 < \sigma < 1.1$  and for Reynolds numbers in the range  $2 < Re_p < 20$ . We show the results of several of our simulations in Fig. 2, together with the results by Zhu (2000), which were obtained by the finite element method for a

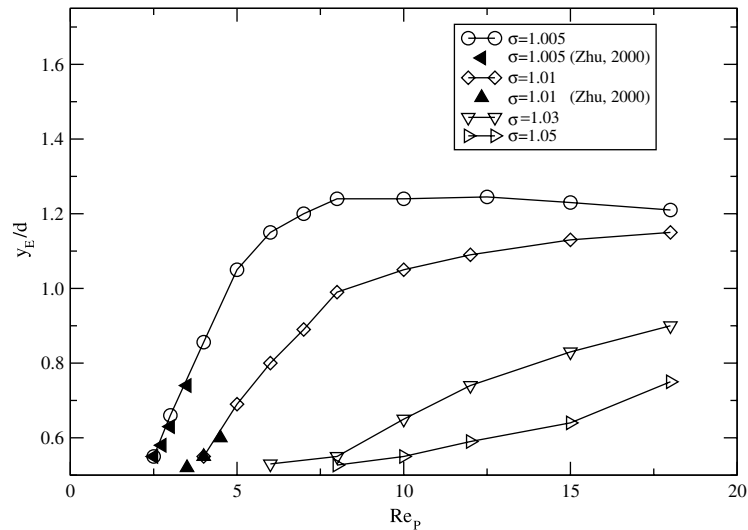


Fig. 2. Equilibrium positions of a particle as a function of the Reynolds number at four different density ratios ( $d/H = 0.1$ ,  $d/W = 0.05$ ).

narrower range of  $Re_p$ . When the center of the particle is at dimensionless height equal to 0.5, then the particle touches the bottom of the flow domain and is not considered suspended. Fig. 2 shows that the lighter particles lift to higher equilibrium positions in the flow domain at relatively low values of  $Re_p$ . Heavier particles settle on the bottom of the flow domain and start being suspended at larger Reynolds numbers. Similar observations were also made for particles in Poiseuille flow by Patankar et al. (2001). It must also be pointed out that, at lower Reynolds numbers, the equilibrium position of the particle is much more sensitive to the particle Reynolds numbers.

An interesting observation in Fig. 2 is that for the very light particles ( $\sigma = 1.005$ ) the equilibrium position appears to reach a maximum and then slightly decreases. This result is further corroborated in Fig. 3, which depicts the trajectories of particles in the  $(x, y)$  plane at four different Reynolds numbers. It is evident that the final equilibrium position at  $Re_p = 12.5$  is slightly higher than the final equilibrium position of a particle at  $Re_p = 15$  and the latter is slightly higher than the equilibrium position at  $Re_p = 18$ . Because this result was unexpected, we conducted a number of grid validation studies to ensure that this observation is not an artifact of the computational grid used or of the relative height of the flow domain and we observed that indeed the numerical value of the equilibrium position becomes slightly lower when  $Re_p > 12.5$ . The difference, although not significant, is of the order of 4%, a number that is higher than the numerical uncertainty of the method used in this study. Also, we found that the particle starts to slightly oscillate around its equilibrium position at  $Re_p = 15$  and 18, with a small amplitude of oscillation. We must point out that the particle Reynolds numbers of the rest of the simulations were not high enough to look for similar results with heavier particles.

The transverse force on the particle is due to the relative rotation of the flow field with respect to the particle. The transverse force is known as the “lift force” or the “Magnus force,” and is the result of an inertial effect that causes a lower pressure on the side of the particle, where the velocity is higher. Saffman computed this force in the case of shear flows and at the limit of very low

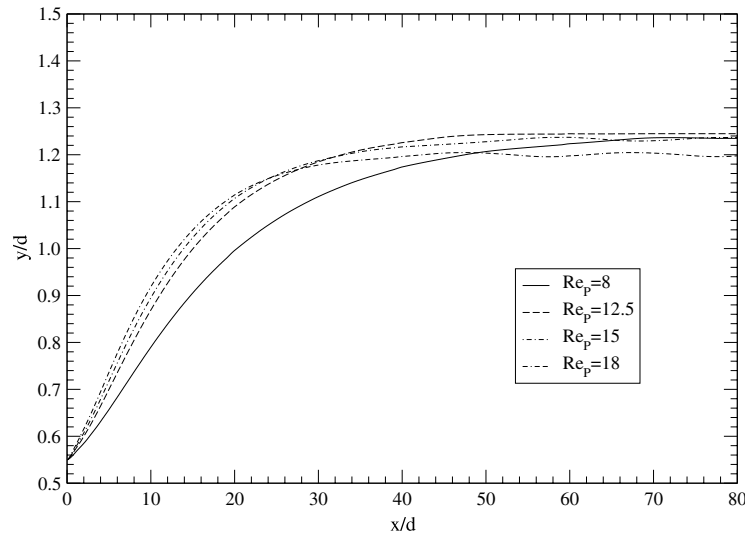


Fig. 3. The trajectories of a particle at different Reynolds numbers for  $\sigma = 1.005$ .

Reynolds numbers and derived a result, which is sometimes called “the Saffman force.” It must be pointed out that both of these “forces” are the manifestation of the same effect, namely that the particle experiences a transverse pressure gradient and, hence, a transverse force when the fluid velocity is higher on the one side than the other. In the case of uniform and symmetric flow around the particle the transverse force vanishes. In the particular case examined here, the transverse force is magnified by the presence of the wall boundary.

In order to investigate the observed maximum in Figs. 2 and 3 we tried to investigate the contribution of the three components of the total lift force exerted on the particle. However, since we do not have a way to compute independently the effect of the wall on the particle, we could only examine the behavior of the lift force when the particle/fluid density ratio is 1.005 and 1.03 respectively. For these calculations we have used a  $600 \times 300$  lattice domain with particle radius equal to 15 lattice units, fluid viscosity  $\mu_f = 0.05$  and density  $\rho_f = 1$ . Because fluctuations over the equilibrium position were observed at  $Re_p = 15$  and 18, we performed computations for at the maximum, minimum and average height of the particles. The results of the computations are shown in Table 1. It is evident that the product  $\omega(U_p - U^\infty)$ , which determines the magnitude of the lift force shows a maximum at approximately  $Re_p = 12.5$  and then drops at a fast rate because the relative velocity of the particle diminishes. We think that this reduction of the lift force is the main reason for the observed maximum of the total lift force in Figs. 2 and 3 for  $\sigma = 1.005$ . In the case of  $\sigma = 1.03$ , all computations show that there is not a comparable decrease in the Magnus force, mainly because the magnitude of the relative velocity remains finite. Because of this, a maximum in the total lift force is not observed at this density ratio.

Fig. 4 shows the particles’ velocity in the vertical direction at  $\sigma = 1.005$ . It is apparent that the particles experience a lift at all three Reynolds numbers and attain their equilibrium positions where the vertical velocity stays at zero ( $Re_p = 8$ ) or exhibits very low amplitude oscillations around zero ( $Re_p = 15$  and 18). This observation is consistent with the results in Fig. 3 and Table 1, which show that the particle slightly oscillates around its equilibrium position at the

Table 1  
Particle velocities and equilibrium position for  $\sigma = 1.005$  and  $\sigma = 1.03$  at different shear Reynolds numbers

$\sigma$	$Re_p$	Equilibrium position, $h_{eq}$	Rotational velocity, $\omega$	Velocity $U_p$	Fluid velocity at $h_{eq}$ , $U^\infty$	$\omega(U_p - U^\infty) \times 10^6$	$\kappa^{1/2}$
1.005	8	1.234d	0.000188	0.01621	0.01645	0.045	0.0211
	12.5	1.245d	0.000286	0.02583	0.02594	0.032	0.0264
	15	1.233d (avg)	0.000336	0.03079	0.03083	0.013	0.0289
	15	1.229d (min)	0.000336	0.03064	0.03073	0.030	0.0289
	15	1.237d (max)	0.000335	0.03093	0.03092	-0.004	0.0289
	18	1.200d (avg)	0.000394	0.03602	0.03601	-0.003	0.0316
	18	1.196d (min)	0.000394	0.03584	0.03588	0.016	0.0316
	18	1.205d (max)	0.000393	0.03620	0.03614	-0.023	0.0316
1.03	8	0.565d	0.000123	0.00470	0.00753	0.344	0.0211
	12.5	0.732d	0.000253	0.01370	0.01525	0.405	0.0264
	18	0.867d (avg)	0.000382	0.02508	0.02600	0.357	0.0316
	18	0.865d (min)	0.000383	0.02499	0.02595	0.369	0.0316
	18	0.868d (max)	0.000381	0.02517	0.02604	0.334	0.0316

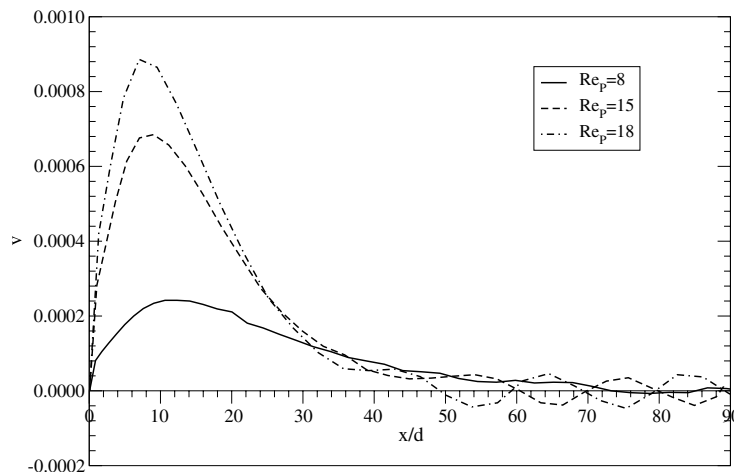


Fig. 4. Particle vertical velocity components at various Reynolds number at  $\sigma = 1.005$ .

higher particle Reynolds numbers. It must be pointed out that Mclaughlin (1993) and Kurose and Komori (1999) observed a drastic reduction of the lift at values of the Reynolds number exceeding 50. In the study by Kurose and Komori (1999) the lift actually becomes negative at the higher values of  $Re_p$ . This drastic reduction on the lift force is mainly due to the flow separation behind the particle. Flow separation has not been observed in this study ( $Re_p$  is too low) but the slight reduction on the lift observed here may be due to the beginning stages of the flow asymmetry, which is apparent in Fig. 5 and, which, at higher  $Re_p$  leads to separation.

Fig. 5 shows the disturbance velocity field created in the shear flow by the presence of the particle at two different Reynolds numbers. The disturbance velocity is defined as the actual

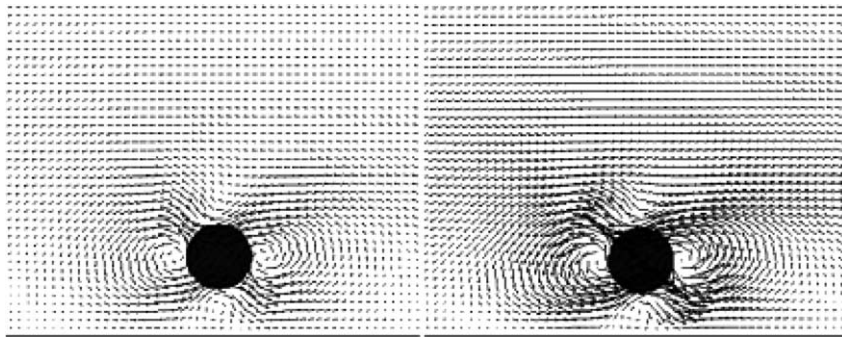


Fig. 5. The disturbance velocity around the particle at (a)  $Re_p = 10$  and (b)  $Re_p = 18$ , both for  $\sigma = 1.005$ .

velocity of the flow field minus the imposed shear velocity. The figure shows the vortices, which are created by the presence of the particle at its upper and lower sides and which contribute to the total lift. It must be pointed out, however, that if these vortices become too strong and the flow separates, the lift decreases drastically (Kurose and Komori, 1999).

Patankar et al. (2001) studied the lift force and equilibrium position of a circular particle in a Poiseuille flow. Fig. 6 shows a comparison of the equilibrium positions for particles in the linear shear flow we examine here and their results for Poiseuille flow. In this case, the size of the computational domain is chosen to be  $H = 12d$  and  $L = 22d$  and the particle-fluid density ratio is 1.01, which is the same as in the simulations of Patankar et al. (2001). Since the shear in a Poiseuille flow diminishes from the boundary to the center of the flow, we have chosen to use the shear at the observed equilibrium position in the study by Patankar et al. (2001) as the (constant) shear of our study. For the particle Reynolds numbers range considered in the two studies, it

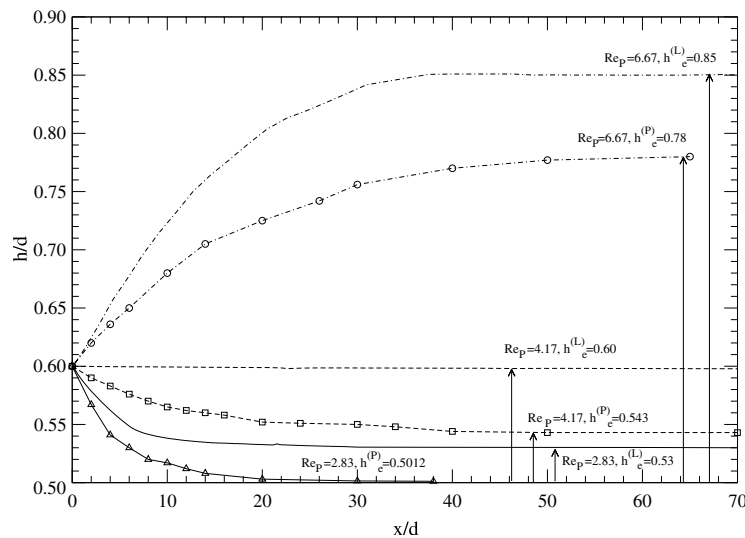


Fig. 6. Equilibrium position at three different shear Reynolds numbers under linear shear flow and Poiseuille flow.



appears that, at the same shear Reynolds number, the particles in the linear shear flow tend to reach higher equilibrium positions. For example, at  $Re_p = 2.83$ , the equilibrium position in the Poiseuille flow is  $0.5012d$  above the channel bottom, while the equilibrium position is about  $0.53d$  for the same particle in a linear flow. This may be due to the fact that the shear is reduced monotonically in Poiseuille flows and, hence, a slight upward departure of the particle from its equilibrium position would result in a decrease of the lift.

In order to investigate the effect of the curvature of the shear function, we considered a case of shear Reynolds number equal to 4.17 in Poiseuille flow. The equilibrium position in this case is  $0.543d$  above the channel bottom. At this equilibrium position, the shear rate at the center of the particle is 91% of the shear rate at the wall. In order to achieve the same ambient shear rate for a particle in a simple shear flow, the corresponding particle shear Reynolds number should be  $Re_p = 3.79$ . We found that the equilibrium position for  $Re_p = 3.79$  in linear shear flow is  $0.57d$ . This observation shows that the curvature of the shear profile tends to decrease the total lift force on the particle.

It is of interest to have a map that delineates when a particle settles at the bottom boundary or remains in suspension at an equilibrium distance from the bottom. For this reason, we have performed computations with the density ratio,  $\sigma$ , and the Reynolds number,  $Re_p$ , as parameters. For the purpose of discriminating settling or suspension of particles, we define that particles that attain an equilibrium position  $y_E/d < 0.52$  (that is, their lowest point is at 0.02 diameter from the bottom surface of the channel), are settled, while particles that attain an equilibrium position higher than 0.52 are suspended. Fig. 7 is a map that shows the results of these simulations. The symbol  $\Delta$  denotes a suspended particles and the symbol  $\nabla$  denotes a settled particle. We have chosen the dimensionless density difference,  $\sigma - 1$ , as the independent variable in this figure, because the driving force of the settling problem for a particle is proportional to the density difference. The dependent variable,  $Re_p$  is a function of the shear rate of the flow. The boundary

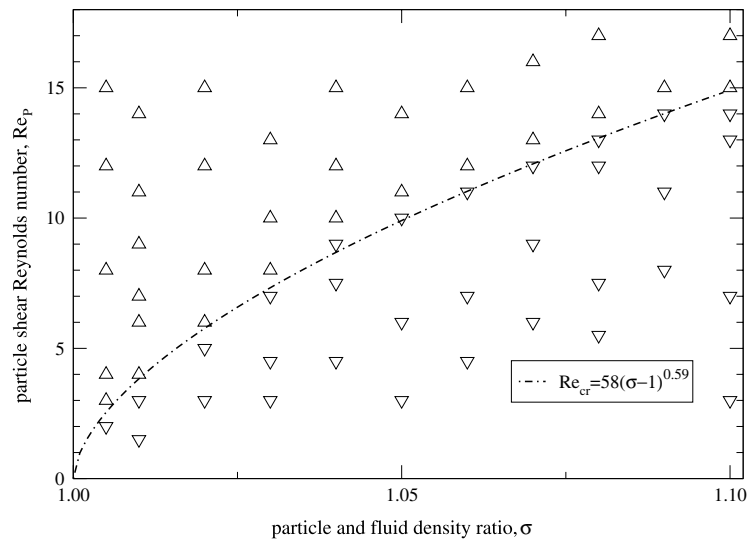


Fig. 7. Settling or suspended particles with  $\sigma$  and  $Re_p$ , as parameters. The symbol  $\Delta$  is for suspended and  $\nabla$  is for settled particles. The curve denotes the correlation equation for the two regions.

that separates the two regions of the symbols  $\Delta$  and  $\nabla$  distinguishes the settling region (lower part of the figure) from the suspension region (upper part of the figure). A correlation equation of this boundary curve may be interpreted as the locus of all the critical shear Reynolds numbers  $Re_p$  needed to lift a particle of density ratio  $\sigma$  is derived based on the simulation data:

$$Re_p = 58(\sigma - 1)^{0.59} \tag{2}$$

Alternatively, the above formula may be written in terms of the gravity Reynolds number, which is a function of the terminal velocity and, hence, of the density difference as follows:

$$Re_G = 0.997 Re_p^{1.69} \tag{3}$$

Patankar et al. (2001) obtained a similar correlation for their computations on Poiseuille flow, which is presented here for comparison:

$$Re_G = 2.3648 Re_p^{1.3904} \tag{4}$$

### 3.2. The effect of the initial position of the particle on the equilibrium position

It must be pointed out that all the data used in Fig. 7 were obtained from numerical computations. The numerical error associated with them is less than the area occupied by the corresponding symbols. We performed several computations in order to determine if the initial position of the spherical particle plays an important role on the equilibrium position and we found that the equilibrium position is unique and does not depend on the initial conditions. This is demonstrated in Fig. 8, which shows the trajectories of a particle with density ratio  $\sigma = 1.01$  at  $Re_p = 10$ , when it is released at three different positions, denoted by  $y_0$ . It is evident that the particle will eventually reach the same equilibrium position, regardless of its initial position. We have also observed that,

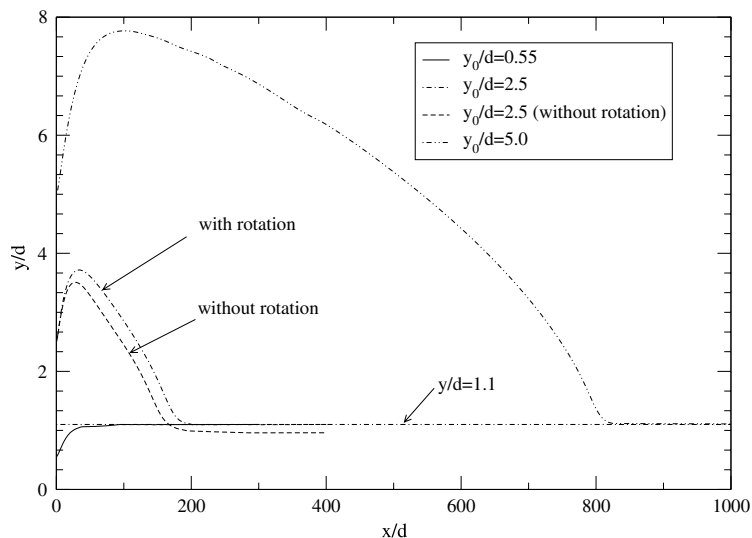


Fig. 8. The trajectories of a particle released at three different locations at  $\sigma = 1.01$  and  $Re_p = 10$ . ( $d/H = d/W = 0.1$ ).

in general, when the particle is released from an initial position, which is higher than the equilibrium position, the initial transient lift force is high enough to move the particle upwards. After the particle translational and rotational velocities reach their equilibrium states in the flow, the particle attains always the same equilibrium position,  $y_E$ , which is independent of its initial position. We have also observed that when the particles are released from below their equilibrium position, then, in general, they rise only to the equilibrium position and they remain at this level. Fig. 8 also shows that the rotation of the particle affects the equilibrium position as shown in the cases of the two particles that are released at  $y_0/d = 2.5$ . One of these particles is allowed to rotate in the flow, while rotation is suppressed in the motion of the other and only translation is allowed. In all our calculations we have observed that the particle rotation always enhances the lift force and allows the particle to reach a higher equilibrium position (because of the Magnus part of the lift force). This is consistent with the findings in studies of particles in Poiseuille flow (Patankar et al., 2001; Joseph, 2002).

### 3.3. Equilibrium positions for particles with a rectangular cross-section

Particles in engineering applications are seldom spherical or cylindrical. For example, a high percentage of the fibers used in the paper and pulp industry have rectangular cross-sections. For this reason it is of interest to study the effect of the shape of the particle on its equilibrium position. In the case of irregular particles it is useful to define a hydraulic diameter as follows:

$$d_h = \frac{4A}{P} \quad (5)$$

where  $A$  is the area of the two-dimensional particle and  $P$  is its perimeter. The hydraulic diameter of a circular cylinder is equal to its proper diameter.

We consider a rectangularly shaped two-dimensional particle with length and width denoted by  $a$  and  $b$  and performed computations for two cases: The first, for  $a = b = 20$ , that is a square shape, and the second for  $a = 2b = 30$ . The hydraulic diameter in each one of these cases is  $d_h = 20$  and this is the same as the diameter of all the circular particles of the previous sections. Fig. 9 shows the trajectories of the rectangularly shaped particles together with that of a spherical particle at  $Re_p = 12$  and  $\sigma = 1.01$ . It is seen that the rectangular particles clearly attain equilibrium positions and that they perform small-amplitude oscillations as they rotate around these positions. It is also observed that the equilibrium position of the square particle is close to that of the circular particle, while the elongated rectangular particle attains a higher position.

It is of interest to note that, because the rectangular particles do not exhibit the same symmetry at any orientation in the flow, their rotation in the flow field creates fluctuations in the hydrodynamic force, which is manifested as fluctuations in the lift and drag components of the force and, finally, as velocity fluctuations. The spherical particle is symmetric and the force exerted on it is constant. Fig. 10, shows the two velocity components of the spherical and the elongated rectangular particle ( $a = 2b = 30$ ) at  $Re_p = 12$ . It is apparent that the particles reach an equilibrium height, since the vertical component of their velocities is very close to zero, with the rectangular particle exhibiting small symmetric fluctuations. A glance at the longitudinal component of the velocity reveals that the drag force on the elongated, rectangular particle is higher than that of the spherical particle and that the longitudinal velocity undergoes small-amplitude fluctuations

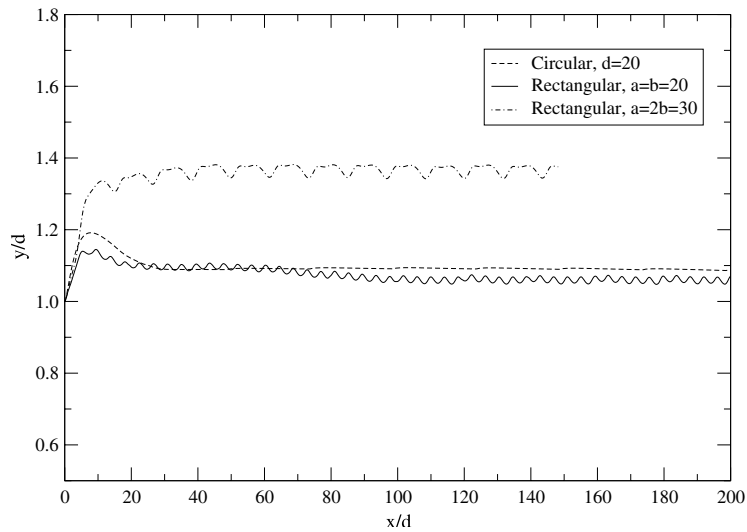


Fig. 9. Trajectories of two rectangular particles at  $Re_p = 12$  and  $\sigma = 1.01$ .

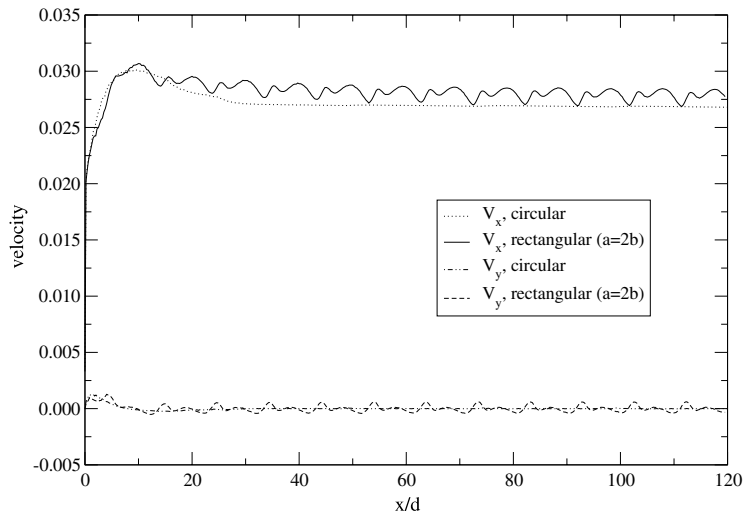


Fig. 10. Velocity components of particles.

around its mean value. The fluctuations are due to the rotation of the elongated particle and the fact that the flow “sees” different frontal areas as this particle translates and rotates.

In the case of a spherical particle, the equilibrium position is independent of how the particle is released. However, we have found out that a rectangularly shaped particle with unequal axes exhibits a behavior that leads to a bifurcation of the value of the equilibrium position. This type of particle may fall and slide along the channel bottom and not lift at all when the initial gap between the particle and the bottom, which is denoted by  $\delta$  here, is less than a critical value. In this case the

long axis of the particle,  $a$ , is parallel to the bottom. This occurs even if the particle is very light and would ordinarily be lifted to a much higher equilibrium position when resuspended. Fig. 10 shows the trajectories of three cases where the same rectangularly shaped particle is released at different positions from the bottom plate:  $\delta/d_h = 0.125$ , 0.158, and 0.292. In these simulations the flow viscosity is chosen to be 0.05 and a finer grid was adopted with the channel width  $L = 600$  and height  $H = 300$ . The velocity on the top plate is  $U_w = 0.3$ ; the length and width of the particle are 45 and 22.5 respectively (this gives the particle hydraulic diameter  $d_h = 30$ ), the shear Reynolds number is 18, and the particle to fluid density ratio is 1.005 (Fig. 11). The results of this bifurcation behavior show that, the critical gap that causes the particle to slide along the channel bottom is between 0.125 and 0.158 hydraulic diameters.

The reason for this behavior of the elongated rectangular particles is that the initial gap between the particle and the bottom plate is very small. Any lifting of the particle would necessitate the filling of this gap with surrounding fluid, which has to rush into the gap. This rushing of the surrounding fluid creates a suction that counteracts the weak lift force developed. This keeps the lower side of the particle close to the bottom, at an equilibrium distance that is determined by the shear rate and the density of the particle.

Fig. 12 shows the particle trajectory in the channel when the particle is released at the three different gaps as specified above. The time step in two consecutive frames is 3000 lattice time units (or  $t^* = 3$ ). The results indicate that when a light rectangularly shaped particle (and most likely other polygonal particles) is approaching the channel bottom, it may be attracted to the bottom and, without making contact with the flat bottom of the channel, it may slide along without being resuspended into the flow again. Running the simulation for a long time convinces that the rectangular particle is not moving away from the wall in a very slow motion. The reason for the parallel motion is that a slight wedge is formed between the rectangle and the flat bottom that provides sufficient suction to counteract the lift and keep the particle in the same vertical position.

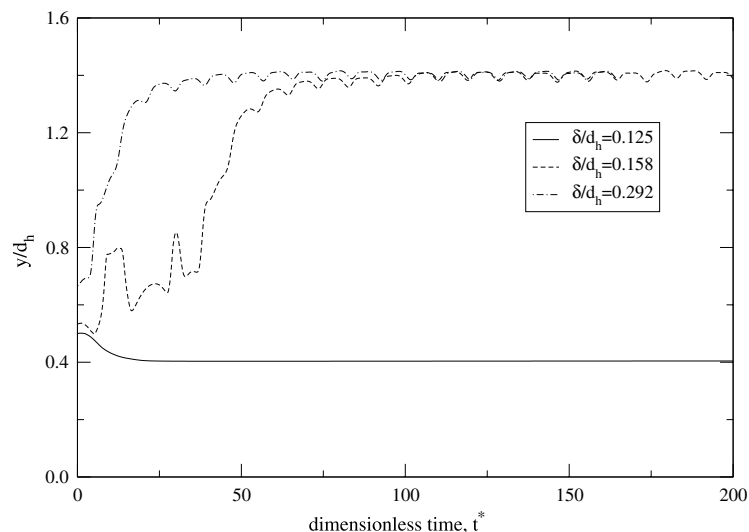


Fig. 11. The vertical position of a rectangular particle for  $Re_p = 18$  and  $\sigma = 1.005$  released at three different positions.

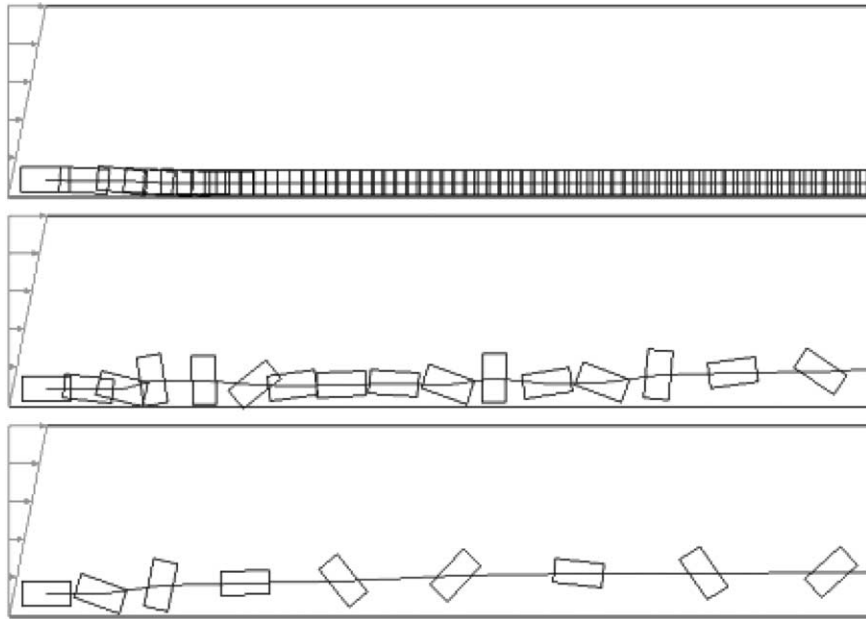


Fig. 12. Particle motions when released at different gaps,  $\delta/d_h = 0.125, 0.158$  and  $0.292$  (there are 3000 iteration steps between two consecutive frames).

Regarding Fig. 12b, the apparent slight penetration of the rectangle on the sixth frame into the boundary is simply an artifact of the graphics. The numerical scheme does not allow any boundary penetration.

#### 4. Conclusions

The combination of the shear lift, the rotational lift and the interactions with the bottom wall, prevent relatively light particles from settling in the bottom of a channel. These particles remain in suspension at an equilibrium position, which is characterized by the equality of the lift forces and the apparent weight of the particle. By using the LBM, we computed the trajectories and determined the equilibrium positions of circular and rectangular particles in simple shear flow, for density ratios up to 1.1 and for particle Reynolds numbers up to 18. It was found that a particle, which in the absence of shear would settle in the bottom of the channel, is actually lifted and remains indefinitely in suspension, close to the bottom of the channel when the Reynolds number is large enough. For example, a particle of density ratio equal to 1.01, remains in suspension when the shear Reynolds number is higher than 5. It is expected that at very high shear rates particles of higher density ratio would remain in suspension. By comparison with those results obtained by Patankar et al. (2001) for Poiseuille flow, we have found that at the same shear Reynolds numbers, particles in linear shear flow are easier to be lifted and reach higher equilibrium positions than that in Poiseuille flow. We have found out that the equilibrium position is independent of the initial position of the particle and that it depends mainly on the particle Reynolds number (defined with

respect to the shear) and the particle to fluid density ratio. Transient effects cause a particle that is released above its equilibrium position to initially rise and then fall back to this equilibrium position. Particle rotation always adds to the lift. In general, rectangularly shaped particles reach equilibrium positions that are higher than spherical particles with the same hydraulic diameters. Because of their lack of symmetry with respect to the flow, the hydrodynamic force, velocities and position of the rectangular particles exhibit small-amplitude fluctuations around their mean values. A light rectangularly shaped particle that is released very close to the flat bottom may be forced to an equilibrium position that is closer to the channel bottom and then slide along the channel bottom in this equilibrium position.

## Acknowledgements

This work was partly supported by three grants from the ONR, DOE and USGS to the Tulane/Xavier Center for Bioenvironmental Research. The authors are thankful for this support.

## References

- Chen, S., Doolen, G.D., 1998. Lattice Boltzmann method for fluid flows. *Ann. Rev. Fluid Mech.* 30, 329–364.
- Feng, Z.-G., Michaelides, E.E., 2002a. Interparticle forces and lift on a particle attached to a solid boundary in suspension flow. *Phys. Fluids* 14, 49–60.
- Feng, Z.-G., Michaelides, E.E., 2002b. Hydrodynamic force on spheres in cylindrical and prismatic enclosures. *Int. J. Multiphase Flow* 28, 479–496.
- Feng, J., Hu, H.H., Joseph, D.D., 1994. Direct simulation of initial value problems for the motion of solid bodies in a Newtonian fluid. Part 2: Couette and Poiseuille flows. *J. Fluid Mech.* 277, 271–301.
- Frisch, U., Hasslacher, B., Pomeau, Y., 1986. Lattice-gas automata for the Navier–Stokes equations. *Phys. Rev. Lett.* 56, 1505–1508.
- Joseph, D.D., 2002. Interrogations of direct numerical simulation of solid–liquid flow. A monograph available on the web site: <<http://www.aem.umn.edu/people/faculty/joseph/>>.
- Joseph, D.D., Ocando, D., 2002. Slip velocity and lift. *J. Fluid Mech.* 454, 263–286.
- Kurose, R., Komori, S., 1999. Drag and lift forces on a rotating sphere in a linear shear flow. *J. Fluid Mech.* 384, 183–206.
- Ladd, A.J.C., 1994a. Numerical simulations of particulate suspensions via a discretized Boltzmann equation. Part 1. Theoretical foundation. *J. Fluid Mech.* 271, 209–285.
- Ladd, A.J.C., 1994b. Numerical simulations of particulate suspensions via a discretized Boltzmann equation. Part 2. Numerical results. *J. Fluid Mech.* 271, 209–285.
- Mclaughlin, J.B., 1993. The lift on a small sphere in wall-bounded linear shear flows. *J. Fluid. Mech.* 246, 249–265.
- Patankar, N.A., Huang, P.Y., Ko, T., Joseph, D.D., 2001. Lift-off of a single particle in Newtonian and viscoelastic fluids by direct numerical simulation. *J. Fluid. Mech.* 438, 67–100.
- Saffman, P.G., 1965. The lift on a small sphere in a slow shear flow. *J. Fluid Mech.* 22, 385–400.
- Segre, G., Silberberg, A., 1961. Radial Poiseuille flow of suspensions. *Nature* 189, 209.
- Segre, G., Silberberg, A., 1962. Behavior of macroscopic rigid spheres in Poiseuille flow. Part 2. Experimental results and interpretation. *J. Fluid Mech.* 14, 136–157.
- Zhu, M.Y., 2000. Direct numerical simulation of the solid–liquid flows of Newtonian and viscoelastic fluids. Ph.D. thesis, University of Pennsylvania.